

Supporting Information

Adjacent Reaction Sites of Atomic Mn₂O₃ and Oxygen Vacancies Facilitate CO₂ Activation for Enhanced CH₄ Production on TiO₂-supported Nickel-hydroxide Nanoparticles

Praveen Kumar Saravanan,^{a,‡} Dinesh Bhalothia,^{b,‡} Amisha Beniwal,^b Cheng-Hung Tsai,^a Pin-Yu Liu,^a
Tsan-Yao Chen,^{b*} Hong-ming Ku,^{c*} Po-Chun Chen,^{a*}

Affiliations:

^a. Department of Materials and Mineral Resources Engineering, National Taipei University of Technology, Taipei 10608, Taiwan.

^b. Department of Engineering and System Science, National Tsing Hua University, Hsinchu 30013, Taiwan.

^c. Chemical Engineering Practice School, King Mongkut's University of Technology Thonburi, Bangkok, Thailand

[‡] Denotes equal contribution of authors.

*Corresponding Author:

Po-Chun Chen

Email: cpc@mail.ntut.edu.tw

Tel: +886-2-27712171 # 2729

FAX: +886-2-27317185

Hong-ming Ku

Email: hongming.ku@gmail.com

Tel: (+662) 470-9616

Fax: (+662) 872-9118

1. Investigation of Gaseous Products

The previously disclosed approach assessed the catalytic behavior of NiMn NCs and experimental nanocatalysts. The control gases were bought from ECGAS Asia and included carbon monoxide (CO) and hydrogen (H₂), in addition to ethane (C₂H₆), propane (C₃H₈), and methane(CH₄) calibrated in He. The gases were injected into sampling rings of varying sizes to obtain varying concentrations of these gases. The varying concentrations of the aforesaid gases were generated by injecting gases into different-sized sampling rings. An automatic blended gas supply device with a heating block was utilized in the research to construct a thermal reaction chamber by packing the specified catalyst inside a glass tube. Glass tube loaded with the catalyst measures 100 millimeters in length, 1 millimeter in width, and 2 millimeters in internal diameter. Using a thermal controller with the PID methodology, the reaction bed temperature can be programmed. Users could form an analytical mechanism with the specific reaction duration, temperature, and flow velocity and remotely start a GC using custom software as the interface by modifying the temperature of the reaction chamber using a thermal regulator with a PID algorithm. An MFC (mass flow controller) was employed to monitor and regulate the gases overall flow rate. Using a GC (gas chromatograph, Agilent 7890, USA) mechanism outfitted with a Valco PDHID detector (model D-3-I-7890, VICI, USA) and a micro and column packed with a carbon molecular sieve (Shincarbon ST, 2 m x 1.0 mm i.d.; Restek Chromatography Products, USA), all gaseous samples originating from the reaction bed were examined. A six-port switching nozzle (A6C6UWT, VICI) from the sampling ring was employed to insert the gas samples into the gas chromatography column to insert a set sample volume (160 mL). Both the discharge and carrier gas are made of ultra-high purity (UHP) helium (99.9995%). And, also the double-heated helium purifiers are located between the flow splitter and cylinder, the main functions of these purifiers are to eliminate the unwanted in the Ultra High Purity helium and to equalize the baseline. The oven temperature has already been from 308 K to 553 K. Finally, take 12 milligrams of the catalyst and blend it with 23

milligrams of silica gel filled with the glass tube. The two ends of the glass tube are shuttered with quartz wool. Before, beginning the experiment, Nitrogen gas was launched into the reactor chamber at room temperature for one hour to eliminate the humidity in the catalyst. In the next step, the pure carbon dioxide and the blended carbon dioxide and hydrogen (1:3) flow into the reaction chamber from 323 K to 573 K range temperature.

2. The HRTEM Images of Control Samples.

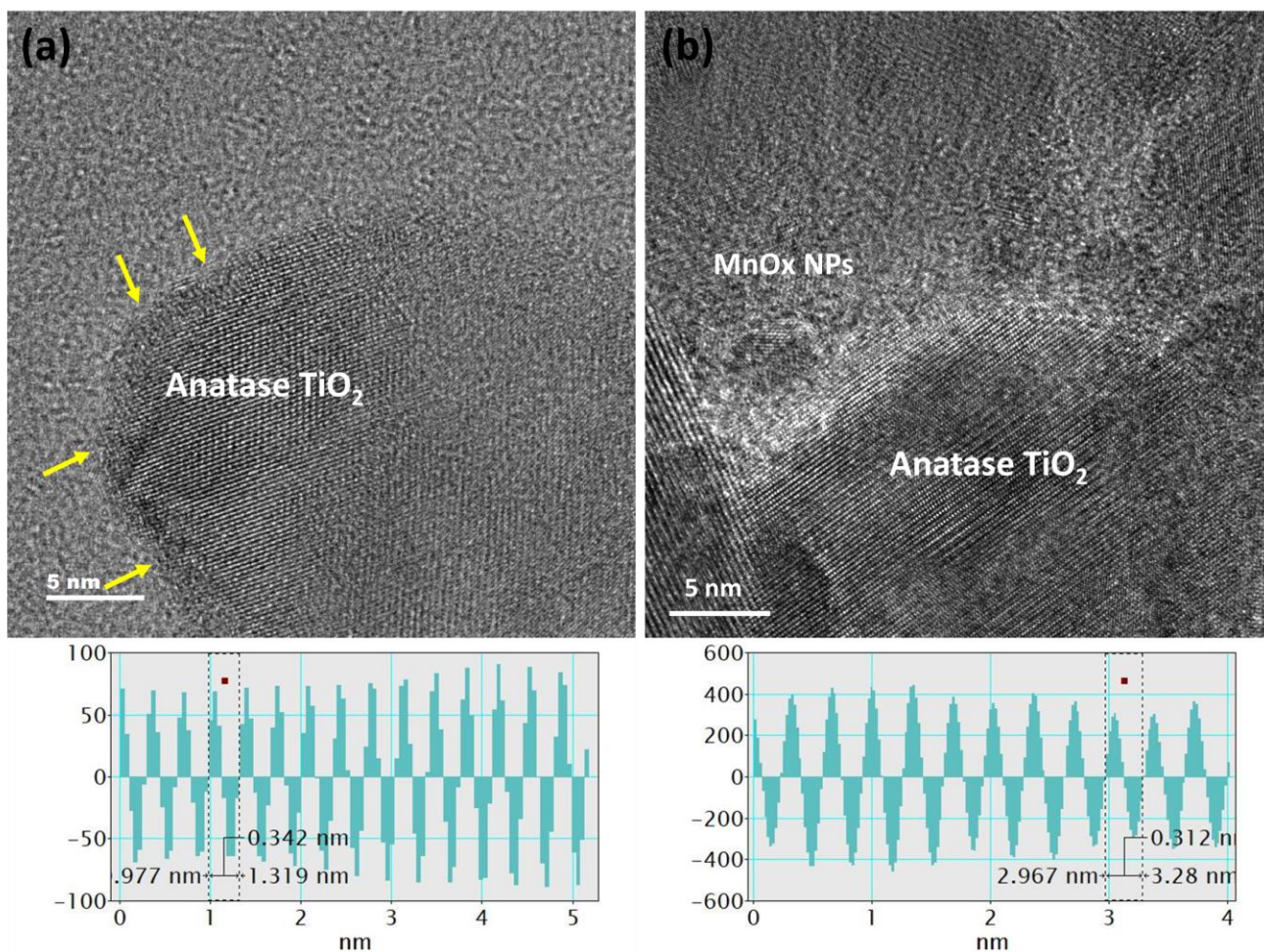


Figure S1. The HRTEM images of (a) P25 and (b) Mn-TiO₂.

3. The Rietveld Refinement Results.

Table S1. Refined lattice parameters and figures of merit from the Rietveld refinement of Mn-TiO₂, Ni-TiO₂, NiMn-1, and NiMn-3 NCs using XRD data.

X	Mn-TiO₂	Ni-TiO₂	NiMn-1	NiMn-3
Anatase Phase TiO₂				
a = b (Å)	3.78577(35)	3.78763(48)	3.78628(38)	3.78874(36)
c (Å)	9.5043(10)	9.5057(15)	9.5058(11)	9.5110(11)
V (Å ³)	136.217(29)	136.370(41)	136.274(32)	136.526(30)
Rutile Phase TiO₂				
a = b (Å)	4.59315(91)	4.5937(14)	4.5940(11)	4.5975(14)
c (Å)	2.9591(11)	2.9597(18)	2.9597(15)	2.9622(18)
V (Å ³)	62.428(34)	62.457(55)	62.465(44)	62.613(54)
Weighted R-profile (Rwp) , R-profile (Rp) and goodness-of-fit (GOF)factors for the S-XRD data histogram				
Rwp (%)	6.52	7.01	4.87	4.93
Rp (%)	5.34	5.59	3.04	3.88
GOF	1.63	2.66	2.13	1.94
Phase Fractions				
Anatase(%)	87.41(47) %	87.24(69) %	87.26(65) %	83.86(78) %
Rutile(%)	12.59(47) %	12.76(69) %	12.74(65) %	16.14(78) %

3. X-ray diffraction pattern of the NiMn catalysts and control samples (after the reaction).

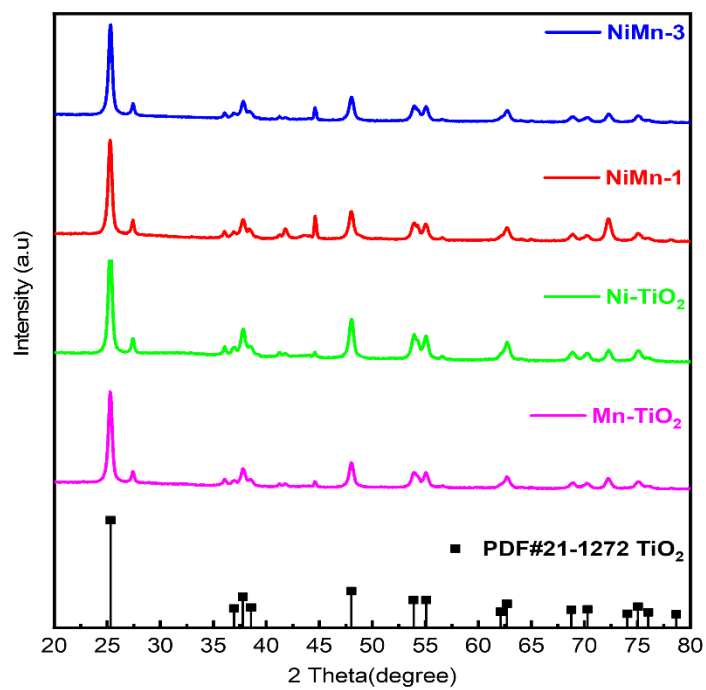


Figure S2. X-ray diffraction pattern of the NiMn catalysts and control samples (Mn-TiO₂, Ni-TiO₂) after the reaction.

4. Model analysis fitting curves compared with experimental FT-EXAFS spectra at Ni K-edge.

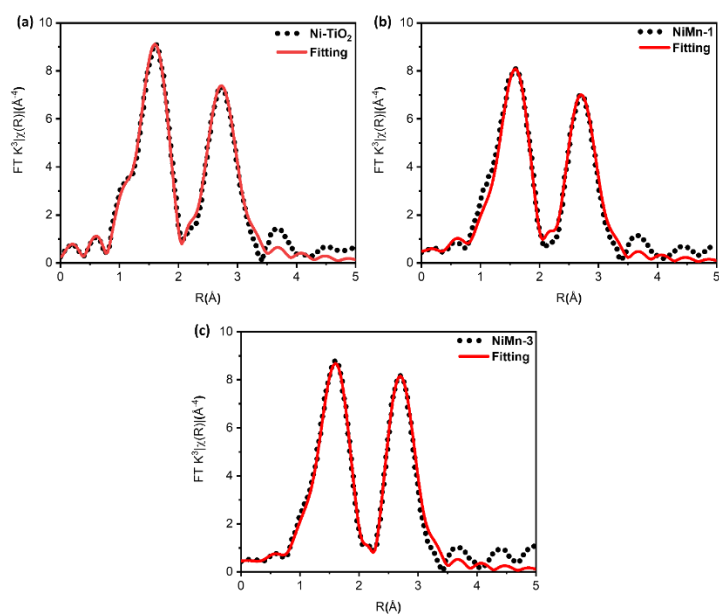


Figure S3. Model analysis fitting curves compared with experimental FT-EXAFS spectra at Ni K-edge of (a) Ni-TiO₂, (b) NiMn-1, (c) NiMn-3 catalysts.

5. Model analysis fitting curves compared with experimental FT-EXAFS spectra at Mn K-edge.

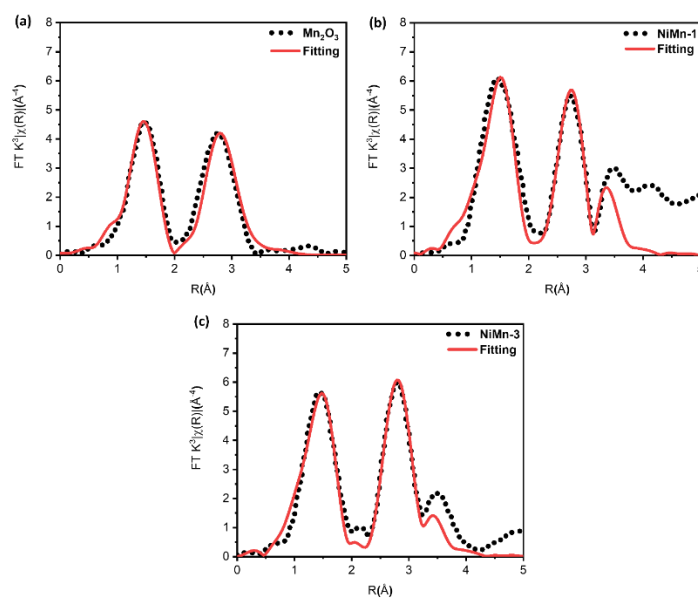


Figure S4. Model analysis fitting curves compared with experimental FT-EXAFS spectra at Mn K-edge of (a) Mn_2O_3 , (b) NiMn-1, and (c) NiMn-3 catalysts.

6. X-ray photoelectron spectroscopy of Ni-TiO₂ at Ni-2p and O-1s orbitals.

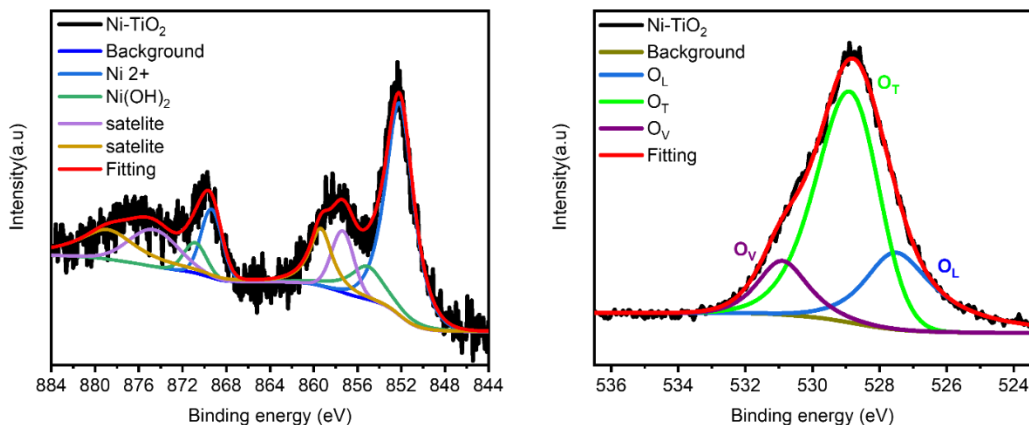


Figure S5. X-ray photoelectron spectroscopy of experimental NC of Ni 2p and O1s orbitals of Ni-TiO₂ NC.

7. XPS determined elemental chemical states and binding energies of experimental NCs.

Table S2. XPS determined the elemental chemical states of experimental samples.

Catalyst	Elemental chemical states (%)						
	Ni ²⁺	Ni(OH) ₂	Mn ³⁺	Mn ⁴⁺	O _L	O _T	O _V
Ni-TiO ₂	79.21	20.79	-	-	25.62	62.34	12.04
NiMn-1	72.66	27.34	37.56	62.44	25.30	45.75	28.96
NiMn-3	76.48	23.52	45.27	54.73	23.58	49.63	26.79

Table S3. XPS determined the binding energies of experimental samples.

Catalyst	Binding energy (eV)						
	Ni ²⁺	Ni(OH) ₂	Mn ³⁺	Mn ⁴⁺	O _L	O _T	O _V
Ni-TiO ₂	852.25	855.15	-	-	527.50	528.90	530.95
NiMn-1	853.20	855.95	635.40	638.90	529.15	530.35	531.95
NiMn-3	853.25	856.90	639.50	641.65	528.50	530.60	532.30

8. Comparison of Selected Catalysts in CO₂ Methanation.

Table S4. The catalytic performance of various catalysts for CO₂ methanation.

Catalysts	Temperature (°C)	Reaction gas	CH ₄ Yield (μmol/g)	CH ₄ selectivity (%)	Reference
NiMn-1	300	CO ₂ : H ₂ = 1: 3	5920	91.9	This study
CPCu-L	300	CO ₂ /H ₂ = 1: 3	404	66.6	[40]
CPCu-03-L			238	N/A	
NiPd-TMOS (NiO _T Pd-T)	300	CO ₂ : H ₂ = 1: 3	1905.1	N/A	[39]
NiO _T -T	300	CO ₂ : H ₂ = 1: 3	1083.2	N/A	
Pd-T	300	CO ₂ : H ₂ = 1: 3	92.2	N/A	
Ru15CaO	400	1.4% CO ₂ + 10% H ₂	414	N/A	[41]
Ru10Na ₂ CO ₃	310	1.4% CO ₂ + 10% H ₂	383	N/A	
CNP-1	300	CO ₂ /H ₂ = 1: 3	202	N/A	[23]
CNP	300	CO ₂ /H ₂ = 1: 3	169	N/A	